HYBRID ATOMISTIC-QUANTUM MECHANICAL SIMULATIONS OF FRACTURE

Rajiv K. Kalia, Aiichiro Nakano, Cindy L. Rountree, and Priya Vashishta
Concurrent Computing Laboratory for Materials Simulations
Department of Physics and Astronomy, Department of Computer Science
Louisiana State University, Baton Rouge, LA 70803

ABSTRACT

A multiscale simulation approach has been developed, which seamlessly combines i) atomistic simulation based on the molecular dynamics method and ii) quantum mechanical calculation based on the density functional theory, so that accurate but expensive computations are performed only where they are needed. Multiscale simulations have been performed to study environmental effects of water molecules on fracture in silicon. Large molecular dynamics simulations have also been performed on parallel computers to investigate dynamic fracture in bulk and nanostructured silica glasses at room temperature and 1,000K. In bulk silica the crack front develops multiple branches and nanoscale pores open up ahead of the crack tip. Pores coalesce and then they merge with the advancing crack-front to cause cleavage fracture. The calculated fracture toughness is in good agreement with experiments. In nanostrucutred silica the crack-front meanders along intercluster boundaries, merging with nanoscale pores in these regions to cause intergranular fracture. The failure strain in nanostructured silica is significantly larger than in the bulk systems.

RESEARCH ACCOMPLISHMENTS

MULTISCALE MOLECULAR DYNAMICS/QUANTUM MECHANICAL SIMULATION OF WATER MOLECULES AT A CRACK TIP IN SILICON

Atomistic simulations are expected to play an important role in scaling down engineering-mechanics concepts — *e.g.*, fracture dynamics based on linear elasticity — to nanometer scales [1]. Recent advances in simulation methodologies and massively parallel computers have made it possible to carry out 10-100 million atom molecular dynamics (MD) simulations of fracture in real materials. However, empirical interatomic potentials used in MD simulations fail to describe chemical processes such as environmental effects on fracture. Instead, interatomic interaction in reactive regions needs to be calculated by a quantum mechanical (QM) method that can describe breaking and formation of bonds. There have been growing interests in developing hybrid MD/QM simulation schemes, in which a reactive region treated by a QM method is embedded in a classical system of atoms interacting via an empirical interatomic potential [2].

An atom consists of a nucleus and surrounding electrons, and QM schemes treat electronic degrees-of-freedom explicitly, thereby describing wave-mechanical nature of electrons. An accurate QM scheme deals explicitly with electronic wave functions, $\psi^{N_{\rm wf}}(\mathbf{r}) = \{\psi_1(\mathbf{r}), \psi_2(\mathbf{r}), ..., \psi_{N_{\rm wf}}(\mathbf{r})\}$ ($N_{\rm wf}$ is the number of independent wave functions, or electronic bands, in the QM calculation), and their mutual interaction in the framework of the density functional theory (DFT) [3, 4] and electron-ion interaction using pseudopotentials [5]. The DFT reduces

the exponentially complex quantum *N*-body problem to a self-consistent eigenvalue problem that can be solved with $O(N_{wf}^3)$ operations. In the DFT scheme, not only accurate interatomic forces are obtained from the Helmann-Feynman theorem, but also electronic information such as charge distribution can be calculated. For efficient parallel implementations, we adopt [6-8] a real-space DFT approach [9], in which wave functions and pseudopotentials are represented on uniform real-space mesh points in Cartesian coordinates. The real-space DFT method is further accelerated by the multigrid method [10, 11]. Parallel implementation of the real-space method is straightforward based on spatial decomposition [6-8].

We have developed a hybrid simulation scheme on parallel computers, in which a QM region is embedded in an atomistic region, see Fig. 1 [12, 13]. The motion of atoms in the QM region is described by a real-space multigrid-based DFT and in the surrounding region with the MD approach. To partition the total system into the cluster and its environmental regions, we use a modular approach based on a linear combination of QM and MD potential energies [14]:

$$E = E_{CL}^{system} + E_{QM}^{cluster} - E_{CL}^{cluster},$$

where $E_{\mathrm{CL}}^{\mathrm{system}}$ is the classical empirical potential energy for the entire system and the last two terms are the QM correction to that energy. $E_{\mathrm{QM}}^{\mathrm{cluster}}$ is the QM energy for an atomic cluster cut out of the total system (its dangling bonds are terminated by hydrogen atoms — handshake H's) and $E_{\mathrm{CL}}^{\mathrm{cluster}}$ is the semi-empirical potential energy of a classical cluster in which handshake H's are replaced by appropriate atoms. In this approach, both QM and MD potential energies for the cluster need be calculated. Termination atoms are introduced in both calculations for the cluster. Handshake atoms linking the cluster and the environment regions are treated by a scaled position method, in which the positions of handshake atoms are determined as functions of the original atomic positions in the system.

The hybrid MD/QM simulation approach has been used to study stress corrosion in silicon. The simulated system is a cracked Si under uniaxial tension with three H_2O molecules around the crack-front, see Fig. 1. The crack surfaces are (110), and the number of the QM atoms near the crack tip is 228 (108 Si and 120 termination-H atoms). The QM region consists of three clusters each containing an H_2O molecule with surrounding Si atoms. The simulation results show significant effects of stress intensity factor, *K*, on the reaction of H_2O molecules at a crack tip in Si. For $K = 0.4\mathrm{MPa}\cdot\sqrt{\mathrm{m}}$, an H_2O molecule either decomposes and adheres to dangling-bond sites on the crack surface (chemisorption) or forms a Si-O-Si structure (oxidation). For a higher *K* value, $0.5\mathrm{MPa}\cdot\sqrt{\mathrm{m}}$, an H_2O molecule either oxidizes or breaks a Si-Si bond.

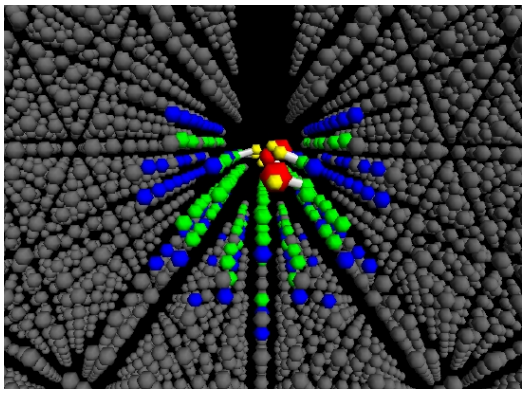

Fig. 1: A close-up of the crack-front region in a hybrid MD/QM simulation of Si. Green spheres represent QM Si-atoms; blue, HS Si-atoms; red, QM O-atoms; yellow, QM H-atoms; gray, MD Si atoms.

MILLION-ATOM MOLECULAR DYNAMICS SIMULATIONS OF DYNAMIC FRACTURE MECHANISMS IN NANOSTRUCTURED SILICA GLASSES

Amorphous silica (a-SiO_2) has a wide range of applications because of its unique chemical and physical properties. The only drawback is it fails in a brittle manner. While brittle fracture in a-SiO_2 has been widely investigated experimentally, only a couple of atomistic simulations have been attempted so far [15]. In particular, little is known about the effect of small grains on fracture and how this behavior contrasts with brittle failure in bulk a-SiO_2. Also, the effect of temperature in these bulk and nanostructured a-SiO_2 systems is not well understood. Recent progress in the development of reliable interatomic interactions, highly efficient algorithms, and massively parallel computers holds a great deal of promise for understanding dynamic fracture in these systems at the atomistic level.

We have performed million-atom MD simulations on crack propagation and fracture in bulk and nanostructured a-SiO_2 systems at room temperature and 1,000K [16]. Molecular-dynamics simulations are performed with an empirical interatomic potential consisting of two-body and three-body terms [17].

Two bulk a-SiO_2 systems containing a million atoms each were prepared by melting β-cristobalite, thermalizing it for 30,000 time steps at 3,500K, and then cooling it gradually to 3,000K where it was again thermalized for 30,000 time steps. Periodic boundary conditions were applied in all the directions. Following this procedure of gradual cooling and thermalization at several intermediate temperatures, the system was brought down to 5K and then subjected to conjugate-gradient quench. This glassy system was heated to 300K, where it was thermalized for 50,000 time steps. Then the temperature was raised to 1,000K and the system was further relaxed for 50,000 time steps.

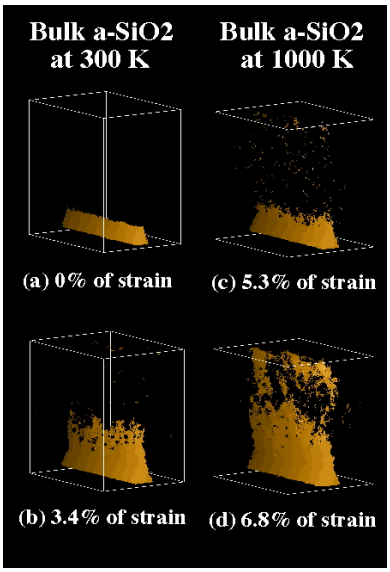

Fig. 2: Snapshots of pores and cracks in bulk a-SiO_2 at 300 K (a) and (b) and 1,000 K (c) and (d). Fig 2(a) shows the initial notch and 2(b) shows its evolution into several branches and nanoscale pores at a strain of 3.4%. The system at 1,000 K shows little progression of the pre-notch even at a strain of 5.3%. However, further increase in strain of 1.5% causes the crack front to move significantly and at the same time several cavities appear as a result of coalescence of nanoscale pores.

The nanostructured systems were prepared by cutting out spheres of radius 40 Å from the bulk amorphous system. These spherical nanoparticles were relaxed with the conjugate-gradient technique and subsequently 100 of these nanoparticules were randomly placed in a MD box. The system was consolidated in the isothermal-isobaric ensemble by gradually increasing the pressure to 16 GPa at 1,000K. Keeping the pressure fixed, the nanostructured system was cooled down to 300K, relaxed for 30,000 time steps, and then the pressure was slowly decreased to zero. This system at zero pressure and 300K has a density of 2.04 g/cc, which is close to the bulk density (2.2 g/cc) [18]. The nanostructured glass at 1,000K was obtained by heating the room temperature nanostructured system to 600K, where it was thermalized for 30,000 time steps, and then the temperature was raised to 1,000K and the system was again thermalized for 30,000 time steps.

In fracture simulations, periodic boundary conditions in x and z directions were removed and uniaxial strain was applied in the z direction by displacing atoms within a cut-off distance of 7.5 Å from the top and bottom layers. In all cases, a triangular notch of length 50 Å and width 40 Å was created by removing atoms along the y direction. The pre-notched systems were strained by displacing boundary-layer atoms by 0.4 Å over a period of 1 ps. Each strained systems was relaxed for 5 ps under isothermal conditions and then the strain was again increased by displacing boundary-layer atoms by 0.4 Å over 1 ps.

Figure 2 shows two sets of snapshots of cracks and pores in bulk a-SiO_2. (Pores were analyzed by dividing a system into voxels of size 5 Å and then identifying empty voxels with common edges or corners). Figure 2(a) displays the initial notch in the system at room temperature. Under strain, the primary crack-front advances and multiple cracks develop inside this front. Concurrently, pores begin to appear mostly ahead of the front, see Fig. 2(b). In the low-temperature system they are closer to the crack-front (within 50 Å) than in the glass at 1,000K (< 100 Å). With an increase in strain, pores grow and coalesce and eventually merge with the advancing multiply branched crack-front. Finally, at a strain of 6.5% this leads to multiple fractures in bulk a-SiO_2 at room temperature. Figures 2(c) and (d) show snapshots of pores and cracks in a-SiO_2 at 1,000K. From Figs. 2(b) and (c), it is evident that the initial notch in the system at 1,000K has advanced much less even though the strain is higher than in the system at room temperature. At 1,000K, pores appear not only in the crack-propagation plane but also in other directions. Pores grow and some of them coalesce with various branches in the advancing crack-front, causing the system to fracture at a strain slightly above 6.8%.

Quantitative analysis of pore growth in the two bulk silica glasses at 300K and 1,000K shows that, up to a strain of 3.5%, they have nearly the same overall porosity, although very different mechanisms of pore formations are involved. At room temperature the increase in porosity is mostly due to crack-front propagation, whereas the front hardly advances at 1,000K. Instead, pores appear ahead of the crack-front in the latter system. With further increase in the strain, the porosity of the room-temperature glass increases much more sharply than that of the system at 1,000K.

Figure 3 shows the effects of strain on crack and pore evolutions in nanostructured a-SiO_2 at 300K and 1,000K. Small pores are found in interfacial regions along nanoparticle boundaries even in the absence of the applied strain. Quantitative analysis shows that pores grow more readily in the low-temperature system as long as the strain is less than 4.5%; above this strain, the pore growth is more prominent in the high-temperature nanostructured system. In both cases, some of the pores merge with the main crack while others coalesce to form secondary cracks ahead of the primary crack. Plateaus alternating with crack growth are also evident in strained nanostructured silica systems. Pre-notches advance above a strain of 2%, followed by plateaus at strains between

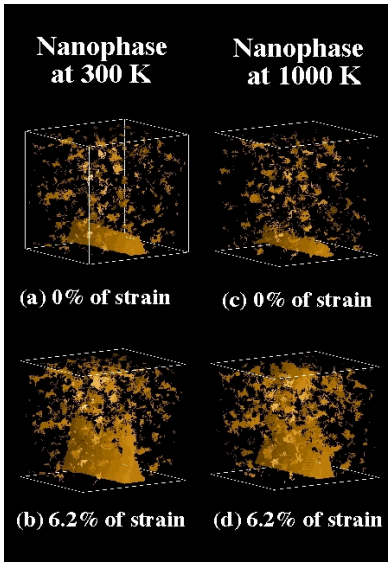

Fig. 3: Snapshots of pores and cracks in nanophase a-SiO_2 at 300 K (a) and (b) and 1,000 K (c) and (d) at the same strain. In (a) and (c) the pores show the interfacial regions between the clusters even without applying a strain. (b) and (d) show the evolution of the crack through the interfacial regions.

3% and 4.5%, and other plateaus at higher strains.

Figures 4(c) and 4(d) show coalescence of a cavity with the main crack and concurrent growth of pores in the nanostructured system. When the strain reaches 9%, the nanostructured systems undergo intergranular fracture. The coalescence of cracks and cavities are also seen in Figs. 4 (a) and (b) for the bulk system at 1,000K, where the circles indicate their locations before and after coalescence. These results provide clear evidence that the strain energies supplied to both bulk and nanostructured systems are dissipated via the growth of pores and since more pores are present in nanostructured systems, the system fractures at higher values of strain than their bulk counterparts.

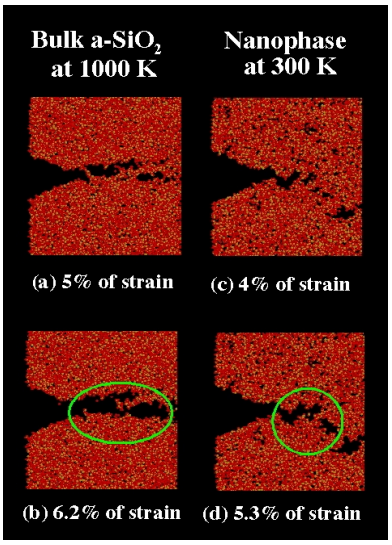

Fig. 4: Snapshots of a close up during the crack propagation in bulk a-SiO_2 at 1,000 K at a strain of 5% (a) and 6.2 % (b) and nanophase at 300 K at a strain of 4 % (c) and 5.3 % (d). In bulk the circle shows the connection between the secondary crack and the main crack. In nanophase, the circle delimitates the region where a cavity merges to the main crack.

Recently we have completed a 15 million-atom simulation of SiO_2. For the 15 million-atom system, we examined the in-plane roughness constant. It was found that the roughness exponent is ~0.5. This is in good agreement with experiments, which state that the results should range from 0.5 to 0.65. Currently we are performing a 115 million-atom simulation of SiO_2.

In summary, these million-atom MD simulations show that advancing crack-fronts in bulk silica develop multiple branches and pores that coalesce among themselves and also with the crack-front. In nanostructured silica glasses pores develop mainly in intergranular regions, crack-fronts meander along intercluster boundaries and they coalesce with pores to cause intergranular fracture. Higher temperature systems have higher porosities and they fracture at higher strains.

REFERENCES

1. P. Vashishta, R. K. Kalia, and A. Nakano, *Comput. Sci. Eng.* **1**(5), 56 (1999).
2. J. Q. Broughton, F. F. Abraham, N. Bernstein, and E. Kaxiras, *Phys. Rev. B*, **60**, 2391 (1999).
3. P. Hohenberg and W. Kohn, *Phys. Rev.* **136**, B864 (1964).
4. W. Kohn and P. Vashishta, in *Inhomogeneous Electron Gas*, eds. N. H. March and S. Lundqvist (Plenum, New York, 1983) p. 79.
5. N. Troullier and J. L. Martins, *Phys. Rev. B* **43**, 1993 (1991).
6. F. Shimojo, T. J. Campbell, R. K. Kalia, A. Nakano, P. Vashishta, S. Ogata, and K. Tsuruta, *Future Generation Computer Systems* **17**, 279 (2000).
7. F. Shimojo, R. K. Kalia, A. Nakano, and P. Vashishta, Comput. Phys. Commun. **140**, 303 (2001).
8. A. Nakano, R. K. Kalia, P. Vashishta, T. J. Campbell, S. Ogata, F. Shimojo, and S. Saini, in *Proceedings of Supercomputing 2001* (ACM, New York, NY, 2001).

9. J. R. Chelikowsky, Y. Saad, S. Ögüt, I. Vasiliev, and A. Stathopoulos, *Phys. Stat. Solidi (b)* **217**, 173 (2000).
10. J.-L. Fattebert and J. Bernholc, *Phys. Rev. B* **62**, 1713 (2000).
11. T. L. Beck, *Rev. Mod. Phys*. **72**, 1041 (2000).
12. S. Ogata, E. Lidorikis, F. Shimojo, A. Nakano, P. Vashishta, and R. K. Kalia, *Comput. Phys. Commun*. **138**, 143 (2001).
13. A. Nakano, M. E. Bachlechner, R. K. Kalia, E. Lidorikis, P. Vashishta, G. Z. Voyiadjis, T. J. Campbell, S. Ogata, and F. Shimojo, *Comput. Sci. Eng*. **3**(4), 56 (2001).
14. S. Dapprich, I. Komáromi, K. S. Byun, K. Morokuma, and M. J. Frisch, *J. Mol. Struct. (Theochem)* **461-462**, 1 (1999).
15. T. P. Swiler, J. H. Simmons, and A. C. Wright, *J. Non-Cryst. Solids* **182**, 68 (1995).
16. C. L. Rountree, R. K. Kalia, E. Lidorikis, A. Nakano, L. Van Brutzel, P. Vashishta, *Annu. Rev. Mater. Res*. **32** (2002) in press.
17. P. Vashishta, R. K. Kalia, J. P. Rino, and I. Ebbsjö, *Phys. Rev. B* **41**, 12197 (1990).
18. T. Campbell, R. K. Kalia, A. Nakano, F. Shimojo, K. Tsuruta and P. Vashishta, *Phys. Rev. Lett*. **82**, 4018 (1999)

ACKNOWLEDGEMENTS

This work was supported by AFOSR and DoD's HPCMO. This work was performed in collaboration with Dr. T. J. Campbell at the Naval Oceanographic Office Major Shared Resource Center, Dr. S. Ogata at Yamaguchi University, Dr. F. Shimojo at Hiroshima University, and Dr. L. Van Brutzel at Louisiana State University. We would like to thank Dr. E. Bouchaud for stimulating discussions and Dr. K. Hideaki for his technical help.